Polyhedron 231 (2023) 116252

Contents lists available at ScienceDirect

Polyhedron

journal homepage: www.elsevier.com/locate/poly

# Synthesis, characterization and photophysical properties of mixed ligand cyclometalated platinum(II) complexes containing 2-phenylpyridine and pyridine carboxylic acids

Evangelia Sifnaiou [a], Antonia Garypidou [a], Konstantinos Ypsilantis [a], John C. Plakatouras [a,b], Achilleas Garoufis [a,b,*]

[a] Department of Chemistry, University of Ioannina, GR-45110 Ioannina, Greece
[b] University Research Center of Ioannina (URCI), Institute of Materials Science and Computing, Ioannina, Greece

ARTICLE INFO

*Keywords:*
Platinum
Cyclometalated
Structure
Fluorescence
2-Phenylpyridine

ABSTRACT

Cyclometalated mixed ligand platinum(II) complexes containing 2-phenylpyridine (ppyH) and pyridine carboxylic acids (PCAs), namely picolinic (2-pyacH), nicotinic (3-pyacH) and isonicotinic (4-pyacH) acid, with the general formula *trans*-N,N-[Pt(ppy)(PCA)Cl] [PCA = 2-pyacH (**2**), 3-pyacH (**3**), 4-pyacH (**4**)] were synthesized and characterized. The crystal structures of the complexes **3** and **4** showed that the PCAs coordinated in a *trans*-position towards the orthometalated ppyC, forming hydrogen-bonded homodimers through their carboxylic groups. NMR spectroscopic techniques were used to identify the solution-structural features of the complexes **2**–**4**. The results revealed that the dihedral angle ($\gamma$) between the PCA plane and the plane of ppy depends on the carboxylic substitution of the pyridine ring and, in the cases of **3** and **4**, the solid-state characteristics were retained. All complexes emit similarly in degassed solution of acetone (475–580 nm) with a very low quantum yield ($\Phi \sim 0.05$–$0.17$ %), while in the solid state, a green emission centered at about 530 nm with $\Phi$ varying from 3.20–4.86 % is produced.

## 1. Introduction

In recent decades, platinum(II) square planar cyclometalated compounds have attracted research interest due to their unique properties of generating radiative emission from triplet states [1]. They have high spin-orbit coupling constants, they are kinetically inert, and their excited state energies can be adjusted through the coordinated ligands [2–5]. Pt(II) complexes with 2-phenylpyridine (ppyH) are unambiguously the most studied in the field [6,7]. PpyH coordinates to the platinum center through the N1 atom of the pyridyl ring and the deprotonated C2 atom of the phenyl group, forming a five-member stable chelate ring enhancing the rigidity of the complex [8]. In addition, a strong ligand field is maintained through the σ-donating C2 atom and the π-accepting N1 of the pyridyl ring. It is noteworthy that the strong field ligands are a crucial factor for the creation of a large gap between the filled $d_{xy}$ and vacant $d_{x^2-y^2}$ platinum orbitals. However, [Pt(ppy)]-based complexes are not always emissive, depending on the nature of the ancillary ligands [9], the modifications on the ppy ring system [10–12], and the various intermolecular interactions such as Pt···Pt, Pt···π (ligand) or ligand π···π stacking [13]. Several emissive {Pt(ppy)}-system complexes exhibit interesting photophysical properties in solid state, attributed to the above interactions which were supported by the ancillary ligands as well. Pyridine carboxylic acids, such as picolinic (2-pyacH), nicotinic (3-pyacH) and isonicotinic (4-pyacH) acid, can form hydrogen bonding networks, $\pi$-$\pi$ stacking interactions and chelate rings or act as bridging ligands through the pyridine nitrogen and the oxygen atom of carboxyl group, resulting in a structurally rich coordination chemistry. [Pt(ppy)]-based complexes with carboxypyridines are rather scarce in the literature. Kato et al. have recently reported on the dependence of the carboxyl group of 2-(*p*-carboxyphenyl) pyridine (HpcppyH) on the photophysical properties of the complex [Pt(HpcppyH)(2-pyacH)] as well as its comparison with the similar of the complexes' emission, arising from their structural differences in solution and solid state. Complexes of the general formula [Pt(ppy)Cl(L)], where L are various derivatives of 2-(2-pyridyl)benzimidazole, have no emissive properties due to their high structural flexibility [14]. Nitrile (NCR) and isocyanide (RNC) ligands (L) complete the Pt coordination sphere of the core {Pt(ppy)Cl} forming the complexes [Pt(ppy)Cl(L)]. The

* Corresponding author at: Department of Chemistry, University of Ioannina, GR-45110 Ioannina, Greece.
*E-mail address:* agaroufi@uoi.gr (A. Garoufis).

https://doi.org/10.1016/j.poly.2022.116252
Received 14 September 2022; Accepted 9 December 2022
Available online 12 December 2022
0277-5387/

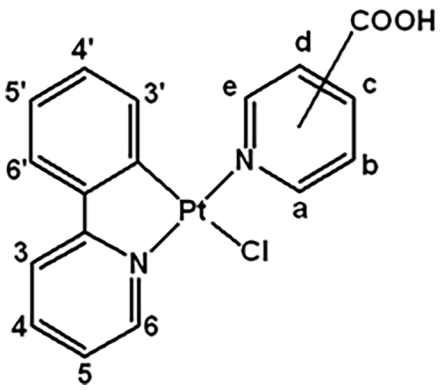


(2) pyridine-2-carboxylic acid (2-pyacH)

(3) pyridine-3-carboxylic acid (3-pyacH)

(4) pyridine-4-carboxylic acid (4-pyacH)

**Scheme 1.** Structure with numbering of the complexes **2**–**4** involved in this study.

emission profile of the complexes in solution showed that CNR and NCR do not contribute significantly to the radiative excited state, which originated from the ppy $^3$LC with a small contribution of $^3$MLCT. In the solid state, the presence of non-covalent interactions differentiates their photophysical properties [15]. The luminescence of the heterobimetallic complexes of the formula [Re(phen)(CO)$_3$($\mu$-aminopyridine)Pt(ppy)Cl]$^{4+}$, in solution at ambient temperature, is caused by the {Re(phen)}-system. However, at low temperature, the emission mainly turns to the $^3$IL state, localized on the metalated ppy ligand, increasing the $^3$MLCT level of the {Re(phen)}-system [16].

Aiming to give insight in the factors affecting the photophysical properties of {Pt(ppy)}-system, herein we report on the synthesis, characterization, and the photophysical properties of a series of complexes with the general formula [Pt(ppy)(PCA)Cl] (PCA = 2-pyacH, 3-pyacH, 4-pyacH) (Scheme 1).

## 2. Experimental

### 2.1. Materials and methods

All solvents were of analytical grade and were used without further purification. 2-phenylpyridine (ppyH), picolinic (2-pyacH), nicotinic (3-pyacH) and isonicotinic (4-pyacH) acids were purchased from Merck Chemical Company and used without further purification. Potassium tetrachloroplatinate(II) (99.9 %) was purchased from Alfa Aesar. The complex [Pt($\mu$-Cl)(ppy)]$_2$was prepared according to the literature methods [17]. High-resolution electrospray ionization mass spectra (HR-ESI-MS) of the compounds were obtained on a Thermo Scientific, LTQ Orbitrap XL™ system. C, H, N determinations were performed on a Perkin-Elmer 2400 Series II analyzer. $^1$H NMR spectra were recorded on Bruker Avance spectrometer operating at proton frequencies of 400.13 and 500.13 MHz and processed using Topspin 4.07 (Bruker Analytik GmbH). Two-dimensional COSY, TOCSY and NOESY spectra were recorded using the standard Brucker procedure and mixing times for the NOESY in the range of 600–800 ms. The $^{13}$C spectra were recorded at 100 MHz and the assignment was assisted by HMQC spectra. The IR spectra of the complexes were recorded on an Agilent Cary 630 FTIR spectrometer. The UV–vis spectra of the complexes were recorded on an Agilent Cary 60 UV–vis spectrophotometer with xenon source lamp, in a solution of acetone for the complexes **1**, **3**, **4** and in a solution of acidified acetone for the complex **2**.

### 2.2. Fluorescence emission studies

The fluorescence emission study was carried out using a Jasco FP-8300 fluorometer equipped with a xenon lamp source. The luminescence quantum yields of the solutions (C = 3.9 × 10$^{-4}$ M) were determined by the equation $Q_s = Q_r(A_r/A_s)(E_s/E_r)(n_s/n_r)^2$, using [Ru(bpy)$_3$]Cl$_2$ in air-equilibrated water solution as a reference standard ($Q_r$ = 0.04). 'A' stands for the absorbance of the solution, 'E' for the integrated fluorescence intensity of the emitted light, 'n' is the refractive index of the solvents and subscripts 'r' and 's' correspond to the reference and the sample respectively. By the equation $Q = S_2/S_0 - S_1$ the quantum yield of solid state of the complexes were calculated. $S_2$ denotes the integrated emission intensity of the sample and $S_0$, $S_1$ stand for the excitation intensities of the standard and the sample respectively.

**Table 1**
Crystal data and structure refinement for $C_{17}H_{13}ClN_2O_2Pt$ (**3**) at 296(2)K and $C_{17}H_{13}ClN_2O_2Pt$ (**4**) at 296(2) K.

| Compound | **3** | **4** |
|---|---|---|
| Empirical formula | $C_{17}H_{13}ClN_2O_2Pt$ | $C_{17}H_{13}ClN_2O_2Pt$ |
| Formula weight | 507.83 | 507.83 |
| Temperature (K) | 296(2) | |
| Wavelength (Å) | 0.71073 | |
| Crystal system | Triclinic | Monoclinic |
| Space group | $P\bar{1}$ | $C2/c$ |
| Unit cell dimensions, $a, b, c$ (Å), $\alpha, \beta, \gamma$ (°) | 11.1941(6), 11.7435(7), 13.2990(7), 76.070(3), 73.074(3), 84.756(4) | 24.071(4), 10.658(2), 14.763(3), 90, 125.583 (6), 90 |
| Volume (Å$^3$) | 1622.91(16) | 3080.3(10) |
| Z | 4 | 8 |
| Density (calc.) (g/cm$^3$) | 2.078 | 2.190 |
| Absorption coefficient (mm$^{-1}$) | 8.820 | 9.294 |
| $F$(000) | 960 | 1920 |
| Crystal size (mm$^3$) | 0.400 × 0.200 × 0.150 | 0.600 × 0.500 × 0.400 |
| Shape | Prism | Parallelepiped |
| Color | Orange | |
| $\theta$ range for data collection (°) | 2.509–25.000 | 3.110–24.999 |
| Index ranges | $-13 \le h \le 13$, $-13 \le k \le 13$, $-15 \le l \le 15$ | $-28 \le h \le 28$, $-12 \le k \le 12$, $-17 \le l \le 17$ |
| Reflections collected | 64,717 | 51,503 |
| Independent reflections | 5723 [$R_{int}$ = 0.0619] | 2715 [$R_{int}$ = 0.0639] |
| Completeness to $\theta$ = 25.000° | 99.8 % | 99.9 % |
| Refinement method | Full-matrix least-squares on F$^2$ | |
| Data/restraints/parameters | 5723/121/409 | 2715/1/213 |
| Goodness-of-fit | 1.042 | 1.066 |
| Final $R$ indices [$I > 2\sigma(I)$] | $R_1$ = 0.0548, w$R_2$ = 0.1394 | $R_1$ = 0.0152, w$R_2$ = 0.0360 |
| $R$ indices [all data] | $R_{all}$ = 0.0662, w$R_{all}$ = 0.1444 | $R_{all}$ = 0.0166, w$R_{all}$ = 0.0364 |
| Largest diff. peak and hole (e·Å$^{-3}$) | 7.444 and −2.692 | 0.592 and −0.854 |

$R = \Sigma||F_o| - |F_c||/\Sigma|F_o|$, $wR = \{\Sigma[w(|F_o|^2 - |F_c|^2)^2]/\Sigma[w(|F_o|^4)]\}^{1/2}$ and $w = 1/[\sigma^2(Fo^2) + (aP)^2 + bP]$ where $P = (Fo^2 + 2Fc^2)/3$ and for **3**: a = 0.0542, b = 43.5134, and **4**: a = 0, b = 11.2959.

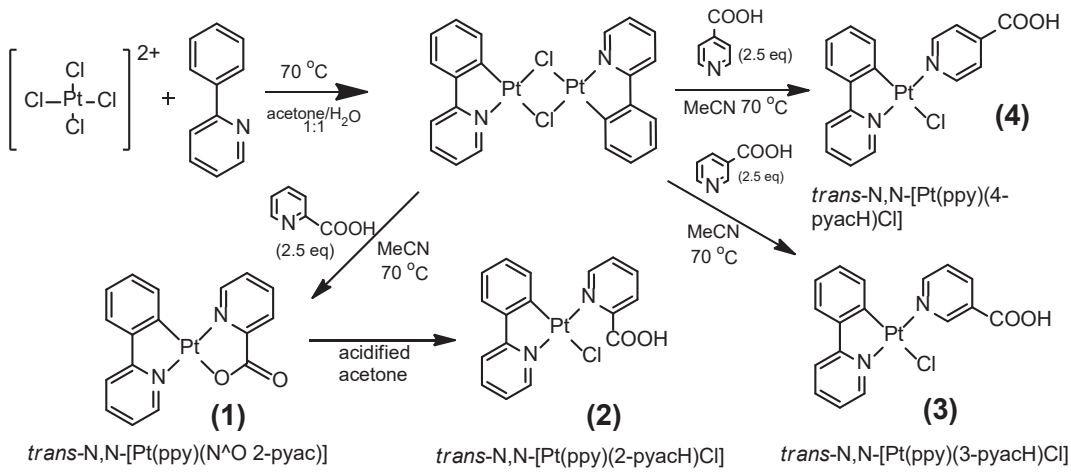


**Scheme 2.** Reactions and conditions for the synthesis of complexes **1**–**4**.

### 2.3. Crystal structure determination

Suitable crystals were glued to a thin glass fiber using cyanoacrylate (super glue) adhesive and placed on the goniometer head. Diffraction data were collected on a Bruker D8 Quest Eco diffractometer, equipped with a Photon II detector and a TRIUMPH (curved graphite) monochromator utilizing Mo Ka radiation (λ = 0.71073 Å) using the APEX 3 software package [18]. The collected frames were integrated with the Bruker SAINT software using a wide-frame algorithm. Data were corrected for absorption effects using the Multi-Scan method (SADABS) [19]. The structures were solved using the Bruker SHELXT Software Package and refined by full-matrix least squares techniques on F2 (SHELXL 2018/3) [20] via the ShelXle interface [21]. The non-H atoms were treated anisotropically, whereas the organic H atoms were placed in calculated, ideal positions and refined as riding on their respective carbon atoms. PLATON [22] was used for geometric calculations, and X-Seed [23] for molecular graphics. Details on data collection and refinement are presented in Table 1 for complex **3** and **4**. Full details on the structures can be found in the CIF files in the ESI. CCDC 2180528 and 2180529 contain the supplementary crystallographic data for this paper. These data can be obtained free of charge via https://www.ccdc.cam.ac.uk/data_request/cif. Hirshfield surfaces and 2D fingerprint plots were calculated and drawn with CrystalExplorer [24].

### 2.4. Synthesis of the complexes

**[Pt(ppy)(2-pyac)] (1):** 24 mg (0.195 mmol) of picolinic acid was added to an acetonitrile solution (5 mL) containing 30 mg (0.039 mmol) of $[Pt(ppy)(\mu\text{-}Cl)]_2$. The reaction mixture was kept at 70 °C for 48 h and then allowed to evaporate slowly. After two days, yellow crystals appeared which were collected by filtration, washed with water (2 × 3 mL) and dried under vacuum over $P_2O_5$. Yield 70 %. $C_{17}H_{12}N_2O_2Pt$: calc. % C, 43.32; H, 2.57; N, 5.94; found C, 43.28; H, 2.66; N, 5.94;. IR, ν(C═O) 1650 $cm^{-1}$. $^1H$ NMR ($CDCl_3$, 298 K, δ in ppm, 500 MHz), H3′, 7.48, (d,1H, $^3J_{Pt\text{-}H}$ = 34.0 Hz, $^3J_{H\text{-}H}$ = 7.7 Hz); H4′, 7.24, (t, 1H); H5′,7.20, (t, 1H, $^3J_{H\text{-}H}$ = 7.4 Hz); H6′,7.54, (d, 1H, $^3J_{H\text{-}H}$ = 7.7 Hz); H3, 7.70, (d, 1H, $^3J_{H\text{-}H}$ = 8.1 Hz); H4, 7.87, (t, 1H, $^3J_{H\text{-}H}$ = 7.7 Hz); H5, 7.17, (t, 1H, $^3J_{H\text{-}H}$ = 6.1 Hz); H6, 9.21, (d,1H, $^3J_{Pt\text{-}H}$ = 39.1 Hz, $^3J_{H\text{-}H}$ = 5.8 Hz); Ha, 9.23, (d, 1H, $^3J_{Pt\text{-}H}$ = 36.1, $^3J_{H\text{-}H}$ = 5.5 Hz); Hb, 7.67, (t, 1H, $^3J_{H\text{-}H}$ = 6.3 Hz); Hc, 8.17, (t, 1H, $^3J_{H\text{-}H}$ = 7.5 Hz); Hd, 8.23, (d, 1H, $^3J_{H\text{-}H}$ = 7.3 Hz). $^{13}C$ NMR ($CDCl_3$, 298 K, δ in ppm, 100 MHz), C1′, 139.6; C2′, 139.4; C3′, 132.1; C4′, 130.0; C5′,122.2; C6′,124.6; $C_2$, 166.9; C3, 118.3; C4, 139.9; C5, 125.6; C6, 150.3; Ca, 148.8; Cb, 127.9; Cc, 139.8; Cd, 128.5; $C_e$, 146.5; COOPt, 154.6. HR-ESI-MS, *m/z* = 472.0619; calc. for $[^{195}PtC_{17}H_{12}N_2O_2]+H^+$, m/z = 472.0630.

**[Pt(ppy)(2-pyacH)Cl] (2):** The complex [Pt(ppy)(2-pyacH)]Cl was formed *in situ* after the dissolution of **1** in 500 μL of acidified acetone-$d_6$ with a drop of DCl 0.01 M and was not isolated. $^1H$ NMR (acetone-$d_6$, 298 K, δ in ppm, 500 MHz), H3′, 6.30, (d,1H, $^3J_{Pt\text{-}H}$ = 41.6 Hz, $^3J_{H\text{-}H}$ = 7.4 Hz); H4′, 6.91, (t, 1H, $^3J_{H\text{-}H}$ = 7.5 Hz); H5′,7.06, (t, 1H, $J_{H\text{-}H}$ = 7.5 Hz); H6′,7.61, (d, 1H, $^3J_{H\text{-}H}$ = 7.9 Hz); H3, 7.92, (d, 1H, $^3J_{H\text{-}H}$ = 8.1 Hz); H4, 7.78, (t, 1H, $^3J_{H\text{-}H}$ = 8.0 Hz); H5, 7.32, (t, 1H, $^3J_{H\text{-}H}$ = 6.5 Hz); H6, 9.62, (d,1H, $^3J_{Pt\text{-}H}$ = 39.5 Hz, $^3J_{H\text{-}H}$ = 6.0 Hz); Ha, 9.32, (d, 1H, $^3J_{Pt\text{-}H}$ = 46.3 Hz, $^3J_{H\text{-}H}$ = 5.6 Hz); Hb, 8.04, (t, 1H, $^3J_{H\text{-}H}$ = 6.7 Hz); Hc, 8.30, (t, 1H, $^3J_{H\text{-}H}$ = 8.0 Hz); Hd, 8.18, (d, 1H, $^3J_{H\text{-}H}$ = 7.8 Hz). $^{13}C$ NMR ($CDCl_3$, 298 K, δ in ppm, 100 MHz), C1′, n.o; C2′, n.o; C3′, 157.3; C4′, 129.7; C5′,120.5; C6′,124.2; $C_2$, n.o; C3, 118.1; C4, 139.3; C5, 127.5; C6, 150.8; Ca, 146.7; Cb, 128.5; Cc, 142.1; Cd, 130.0; $C_e$, n.o; COOH, n.o. HR-ESI-MS, m/z = 508.0366 calc. for $[^{195}PtC_{17}H_{12}N_2O_2Cl]$, m/z = 508.0391.

**[Pt(ppy)(3-pyacH)Cl] (3):** In a 10 mL vial, an amount of 30 mg (0.039 mmol) of $[Pt(\mu\text{-}Cl)ppy)]_2$ was dissolved in 5 mL of acetonitrile and then 24 mg (0.195 mmol) of nicotinic acid ($C_6H_5NO_2$) was added. The mixture was left to react for 48 h at 70 °C in the closed vial. The yellow crystals were collected with filtration, washed with water (2 × 3 mL) and dried under vacuum over $P_2O_5$. Yield 70 %. $C_{17}H_{13}N_2O_2ClPt$: calc.% C, 40.21; H, 2.58; N, 5.52. Found C, 40.40; H, 2.73; N, 5.39. ν(C═O) 1691 $cm^{-1}$. $^1H$ NMR (Acetone-$d_6$, 298 K, δ in ppm, 500 MHz), H3′, 6.39, (d,1H, $^3J_{Pt\text{-}H}$ = 41.0 Hz, $^3J_{H\text{-}H}$ = 7.7 Hz); H4′, 6.97, (t, 1H, $^3J_{H\text{-}H}$ = 7.6 Hz); H5′, 7.09, (t, 1H, $^3J_{H\text{-}H}$ = 7.7 Hz); H6′, 7.66, (d, 1H, $^3J_{H\text{-}H}$ = 8.1 Hz); H3,7.97, (d, 1H, $^3J_{H\text{-}H}$ = 8.7 Hz); H4, 7.83, (t, 1H, $^3J_{H\text{-}H}$ = 8.1 Hz); H5, 7.36, (t, 1H, $^3J_{H\text{-}H}$ = 6.9 Hz); H6, 9.70, (d,1H, $^3J_{Pt\text{-}H}$ = 38.0 Hz, $^3J_{H\text{-}H}$ = 5.8 Hz); Ha, 9.52, (s, 1H, $^3J_{Pt\text{-}H}$ = 48.3 Hz); Hc, 8.65, (d, 1H, $^3J_{H\text{-}H}$ = 5.8 Hz); Hd, 8.06, (t, 1H, $^3J_{H\text{-}H}$ = 6.4 Hz); He, 9.21, (d, 1H, $^3J_{Pt\text{-}H}$ = 45.4 Hz, $^3J_{H\text{-}H}$ = 7.9 Hz). $^{13}C$ NMR (Methanol-$d_4$, 298 K, δ in ppm, 100 MHz), C1′, 146.2; C2′, 140.0; C3′,133.7; C4′, 131.8; C5′,126.1; C6′,125.3; C2, 165.6; C3, 120.5; C4, 142.0; C5, 124.0; C6, 149.3; Ca, 155.7; $C_b$,132.0; Cc, 141.3; Cd, 128.3; Ce, 157.6; COOH, 167.7. HR-ESI-MS, positive (m/z): found. 472.0613, calc. 472.0619 for $[^{195}PtC_{17}H_{13}N_2O_2]$.

**[Pt(ppy)(4-pyacH)Cl] (4):** Complex **4** was prepared in a similar manner to **3**. Yield 60 %. $C_{17}H_{13}N_2O_2ClPt$: calc.% C, 40.21; H, 2.58; N, 5.52. Found C, 40.30; H, 2.68; N, 5.42. ν(C═O) 1695 $cm^{-1}$.$^1H$ NMR (Acetone-$d_6$, 298 K, δ in ppm, 500 MHz), H3′, 6.42 (d,1H, $^3J_{Pt\text{-}H}$ = 44.3 Hz, $^3J_{H\text{-}H}$ = 7.7 Hz); H4′, 6.97, (t, 1H, $^3J_{H\text{-}H}$ = 7.4 Hz); H5′, 7.08, (t, 1H, $^3J_{H\text{-}H}$ = 7.9 Hz); H6′, 7.66, (d, 1H, $^3J_{H\text{-}H}$ = 7.4 Hz); H3, 7.97, (d, 1H, $^3J_{H\text{-}H}$ = 7.9 Hz); H4, 8.05, (t, 1H, $^3J_{H\text{-}H}$ = 7.1 Hz); H5, 7.36, (t, 1H, $^3J_{H\text{-}H}$ = 7.2 Hz); H6, 9.70, (d, 1H, $^3J_{Pt\text{-}H}$ = 36.5 Hz, $^3J_{H\text{-}H}$ = 5.7 Hz); Ha/He, 9.21, (d, 2H, $^3J_{Pt\text{-}H}$ = 43.5 Hz, $^3J_{H\text{-}H}$ = 6.8 Hz); Hb /Hd, 8.11 (d, 2H, $^3J_{H\text{-}H}$ = 6.7 Hz). HR-ESI-MS, positive (m/z): found. 472.0615, calc. 472.0619 for $[^{195}PtC_{17}H_{13}N_2O_2]$.

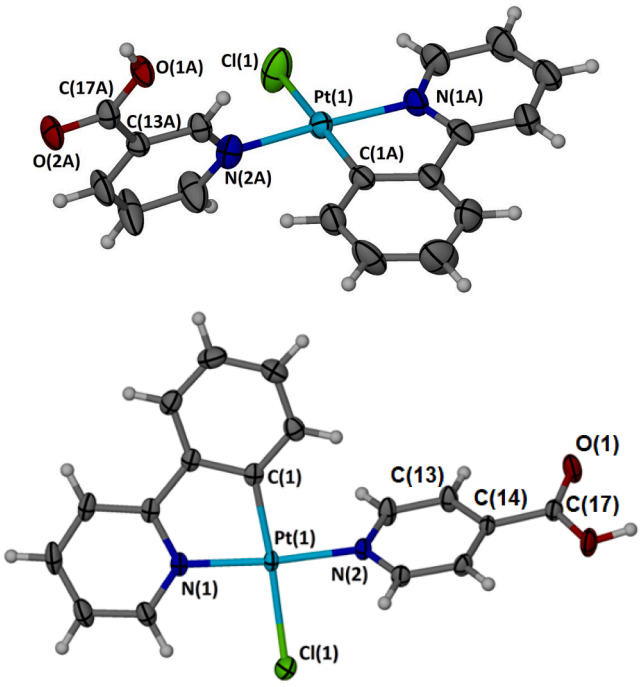


**Fig. 1.** Partially labeled thermal ellipsoid plots (50 % probability level) of molecule **3(a)** and **4(b)**. Selected bond distances (Å) and angles for a) **3**A: Pt (1)–C(1A) 1.974(10), Pt(1)–N(2A) 2.016(11), Pt(1)–N(1A) 2.030(10), Pt(1)–Cl (1) 2.402(4); C(1A)–Pt(1)–N(2A) 90.5(4), C(1A)–Pt(1)–N(1A) 83.3(4), N(2A)–Pt(1)–N(1A) 173.5(5), C(1A)–Pt(1)–Cl(1) 173.4(4), N(2A)–Pt(1)–Cl(1) 90.2(3); b) **4:** Pt(1)–C(1) 1.988(3), Pt(1)–N(1) 2.018(2), Pt(1)–N(2) 2.028(2), Pt(1)–Cl (1) 2.3988(10); C(1)–Pt(1)–N(2) 94.00(12), C(1)–Pt(1)–N(1) 81.38(12), N(1)–Pt(1)–N(2) 173.62(10), C(1)–Pt(1)–Cl(1) 174.81(9), N(2)–Pt(1)–Cl(1) 89.65(8), N(1)–Pt(1)–Cl(1), 95.26(8).

## 3. Results and discussion

### 3.1. Synthesis of the complexes

All complexes were synthesized through the reaction of the dimer [Pt($\mu$-Cl)(ppy)]$_2$ with the pyridine carboxylic acids (2-pyacH, 3-pyacH, 4-pyacH) at a molar ratio of 1:2.5. The complexes **3** and **4** were assigned to the formula [Pt(ppy)(PCA)Cl] (PCA = 3-pyacH, 4-pyacH), while complex **1** was structurally characterized by Ebina et al., as [Pt(ppy)(2-pyacH)] [10]. The reactions between nicotinic acid (3-pyacH), isonicotinic acid (4-pyacH) and [Pt($\mu$-Cl)(ppy)]$_2$ were performed in acetonitrile (Scheme 2). In the case of picolinic acid (2-pyacH), complex **1** was formed followed by the deprotonation of the 2-pyacH carboxylic group. After the dissolution of **1** in acidified acetone-$d_6$, with DCl, the complex [Pt(ppy)(2-pyacH)Cl], (**2**), was formed, as confirmed by the $^1$H NMR and HR-ESI-MS spectra. All attempts to isolate it in solid state through precipitation or crystallization were unsuccessful since it appears that complex **2** exists only in acidic solutions. Scheme 2 summarizes the reaction and the conditions of the synthesized complexes.

### 3.2. X-ray crystal structure of complexes 3 and 4

Complex **3** crystallizes in the triclinic crystal system and $P\bar{1}$ space group with two slightly different molecules in the asymmetric unit (denoted as A and B). Only one of them (A), will be described in detail. A thermal ellipsoid plot is presented in Fig. 1(a).

The geometry around the platinum center is distorted square planar (*sp*) and the coordination sphere consists of the ppy atoms C(1) and N(1), the N(2) of 3-pyacH, and a Cl(1) which is in *trans* position to orthometalated ppy C(1). The chelation of ppy forms a five membered chelate ring causing remarkable distortion from the ideal *sp* geometry with a bite angle C(1A)–Pt–N(A), 83.3(4)° and C(1B)–Pt(2)–N(1B), 86.9(4)°.

The bond lengths are within the range of similar complexes [25,26], however the Pt–Cl bond length is among the longest (Pt(1)–Cl(1A) = 2.400(4) Å, Pt(2)–Cl(2A) = 2.401(5) Å) reflecting the *trans*-influence of the σ-donating ppy C(1) [9,23]. The dihedral angle between the ppy and 3-pyacH is 77.00° for A and 83.48° for B, indicating an almost vertical orientation between the ppy and 3-pyacH planes. The coordination spheres of both A and B are essentially planar with the larger deviation of the calculated least squares planes being 0.094 and 0.057 Å for ClA and ClB respectively for A and B. The carboxylate group of the 3-pyacH is slightly twisted, with a torsion angle O(1A)–C(17A)–C(13A)–C(12A) of 3.41(1)°. The ppy, pyridine and phenyl aromatic rings are coplanar, with the maximum deviation from the calculated least squares plane being 0.055 and 0.081 Å respectively for A and B. Both molecules of **3** in the unit cell (A and B) form hydrogen-bonded homo-dimers (shown in Fig. 2) through their carboxylic groups with donor-H-acceptor (D–H–A) distance for **3**A O(1A)–O(2A)#1, 2.595(15) Å and for **3**B, O(1B)–O(2B) #1, 2.577(15) Å. In the crystal structure of 3-pyacH [27] the molecules are connected in chains through hydrogen bonds between the oxygen atom of the carboxylic group and the nitrogen atom of the pyridine of the next molecule. However, 6-chloronicotinic acid (6-Cl 3-pyacH) forms centrosymmetric dimers through intermolecular hydrogen bonds between its carboxylic groups [28].

The D–H···A distance for the 6-Cl 3-pyacH was measured as 2.6382 (14) Å, slightly longer than that of 3-pyacH in complex **3**. In addition, weak intramolecular interactions between the Cl(1) and the neighboring H(11) of the ppy pyridine ring were observed with a D···A distance Cl (1)–C(11A) = 3.298(1) Å and Cl(1)–C(11B) = 3.287(1) Å. Stacking interactions between the ppy ring system were observed (Fig. S1).

Alternating H-bonding and stacking interaction led to the formation of 1D chains running parallel to the (0, 1, 1) dimension of the unit cell, for both molecules **3**A and **3**B (Fig. S2).

There is a second topological scenario for the description of the network formed in the crystal structure of **3** which leads to a 2D supramolecular architecture. It involves the formation of tetranuclear arrangements via non-conventional C–H···Cl hydrogen bonds. Those

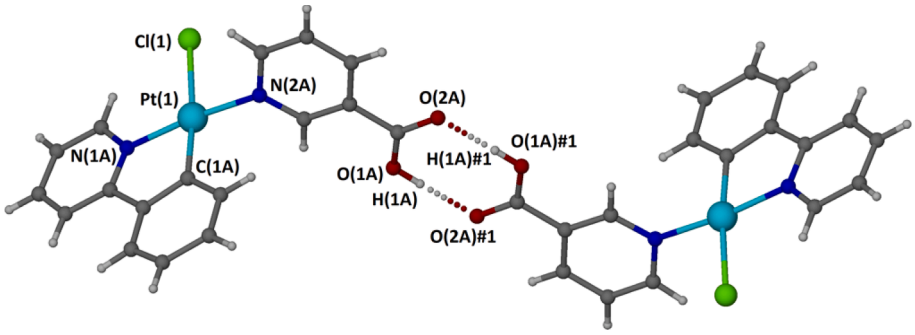


**Fig. 2.** The H-bonded homodimer between A molecules of compound **3**. Symmetry operation to generate equivalent atoms: #1, −x + 1, −y + 1, −z.

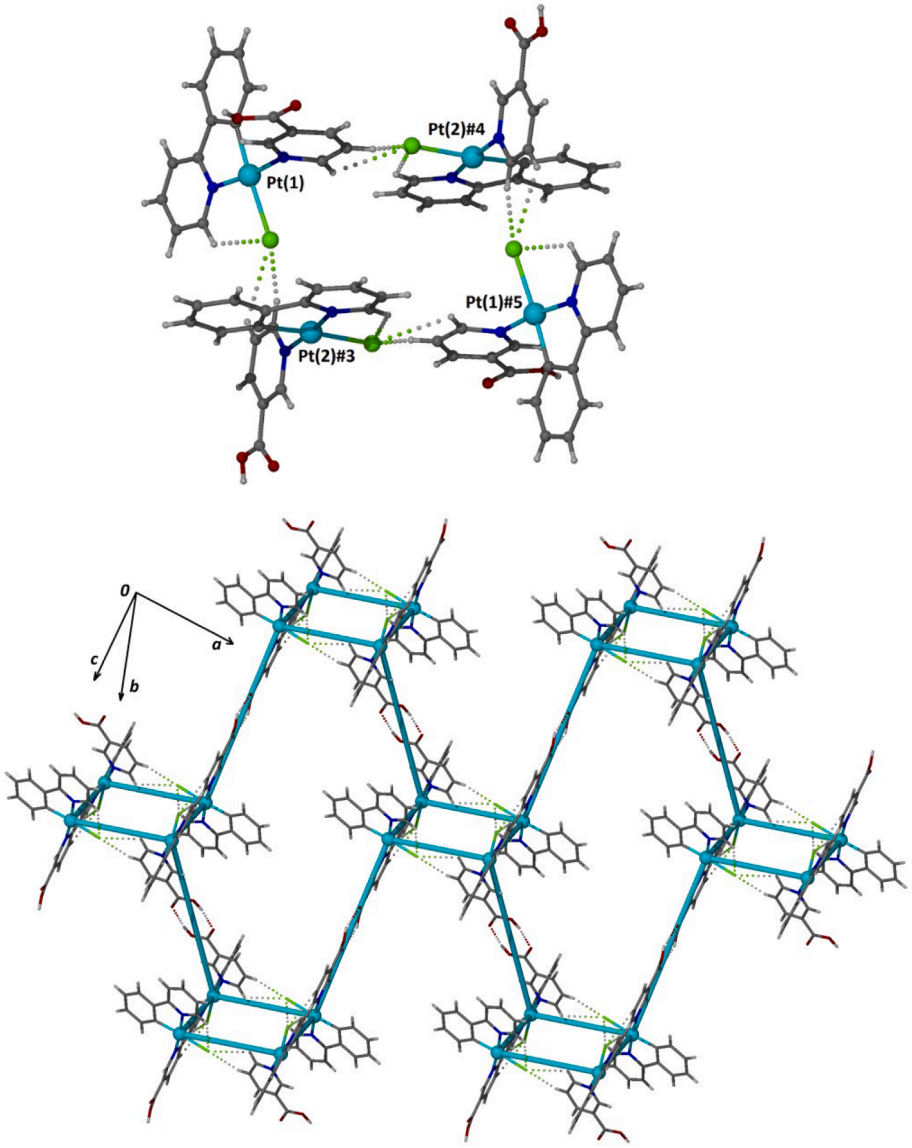


**Fig. 3.** A topological description for the network of compound **3**. Top: The tetranuclear unit formed through non-conventional hydrogen bonding interactions. Symmetry operations to generate equivalent atoms: #3, x, y + 1, z; #4, −x + 2, −y + 1, −z; #5, −x + 2, −y + 2, −z. Bottom: The undulating layer with **fes** topology and point symbol [$4.8^2$] formed by utilization of the carboxylate hydrogen bonds.

tetranuclear arrangements can be considered as nodes and each one interact with four symmetry related groups via the carboxylate hydrogen bonds resulting in a **fes** (according to Reticular Chemistry Structure Resource) 2D network (as shown in Fig. 3) with point symbol [$4.8^2$] (TOPOSPro [29]). The closest Pt···Pt distance for **3** is 6.239(5) Å eliminating the possibility of a Pt–Pt bond.

The interactions between the constituents of the unit cell, apart from the hydrogen bonds and the stacking interactions, are rather

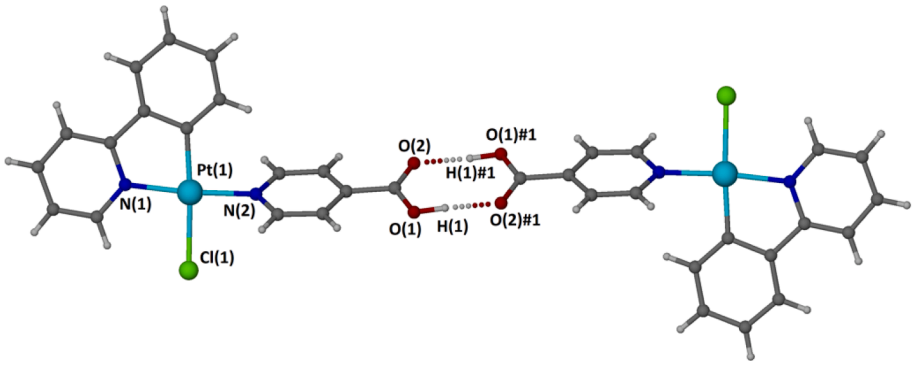


**Fig. 4.** The H-bonded pair in the structure of **4**. Symmetry operation to generate equivalent atoms: #1, −x + 1, −y, −z + 1.

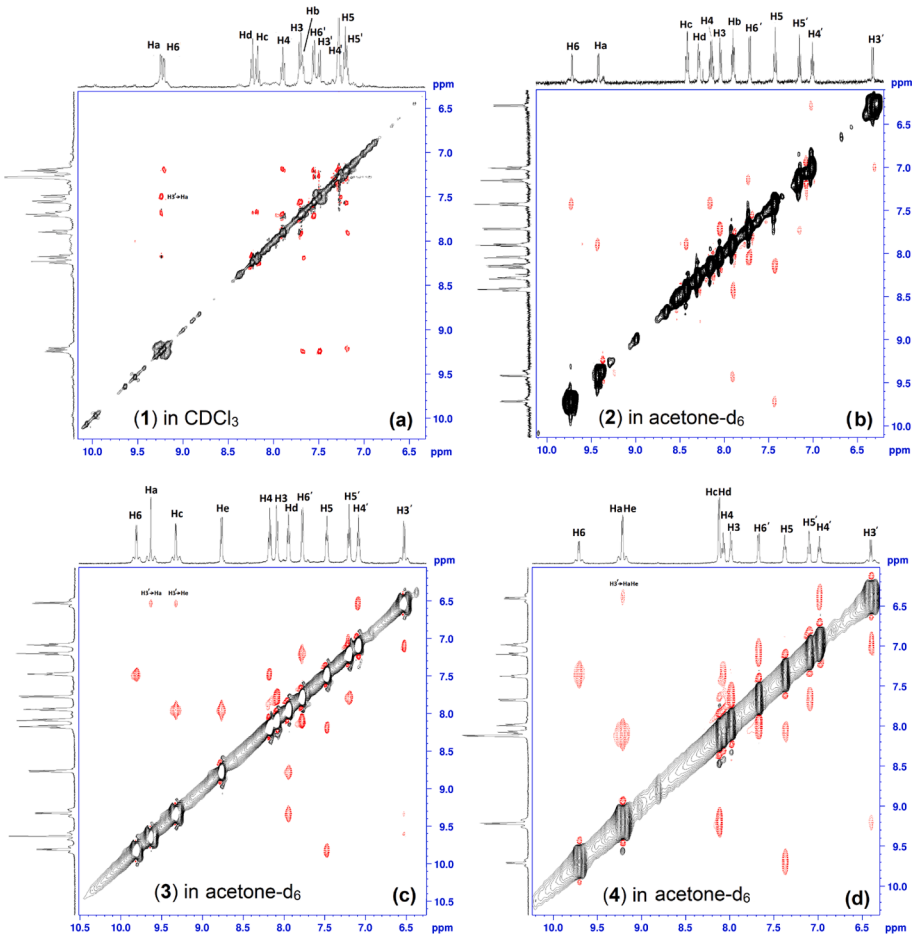


**Fig. 5.** Aromatic part of the NOESY spectra ($\tau_{mix}$ = 600 ms, 298 K) of the complexes **1**–**4** with proton assignments showing the intraligand NOE connectivity of ppyH3′ and the 2-pyacHa, 3-pyacHa, 4-pyacHa.

complicated since there are quite a few unconventional interactions. Since Hirshfeld surface calculations are rather popular today to evaluate molecular contacts in the solid state, we used Crystal Explorer [24]. In this context, two parameters are described when getting a molecular Hirshfeld surface. $d_e$ is the distance from the surface to the nearest atom outside of the surface and $d_i$ is the distance corresponding to the nearest atom inside of the surface. $d_{norm}$ value is dependent on $d_e$, $d_i$, and van der Waals radii. The color of the surface is red when the distance is smaller than the sum of the van der Waals radii and blue when larger. In addition, the 3D Hirshfeld surface can be converted into 2D fingerprint plots using $d_i$ and $d_e$ distances [30]. The Hirshfeld surface of **3** with related fingerprint plots are presented in Fig. S5. As can be seen in Fig. S5a, the strong H-bond acceptor (red color) areas are limited close to oxygen atoms. The closest acceptor···H interactions are attributed to the C–H···Cl non-conventional interactions (see Fig. S5e) while the C···C contacts are limited (compare Fig. S5c with d and e). The H···H contacts dominate the surface, being 42.4 % of the total surface.

Fig. 1b presents a thermal ellipsoid plot for complex **4**. The geometry around the platinum center is distorted square planar (*sp*) and the coordination sphere consists of the ppy atoms C(1) and N(1), the N(2) of 4-pyacH and completed by Cl(1), *trans* to ppyC(1) as in complex **3**. The bond distances are within the range of similar complexes [10], while the Pt–Cl bond length is among the longest [Pt(1)–Cl(1) = 2.3988(10) Å]. As in complex **3** the coordination sphere of **4** is planar with the largest deviation from the last squares' plane for C(1) (0.082 Å). The dihedral angle between the ppy and 4-pyacH planes is 65.52°, deviating significantly from the vertical position in comparison to **3**. The carboxylate group of the 4-pyacH is slightly twisted, with the torsion angle O(1)–C(17)–C(14)–C(13) = 9.6(2)°.

Complex **4** forms hydrogen-bonded dimers through the carboxylic groups (Fig. 4) with D···A distance O(1)–O(2)#1, 2.693(4) Å which is similar with other hydrogen-bonded dimers such as $[Ni(SCN)_2(4\text{-pyacH})_2]\cdot 1/2C_{14}H_{10}$ [31] (Fig. 4). In addition, weak intramolecular interactions between the Cl(1) and the neighboring H(2) of the ppy pyridine ring were observed with a D···A distance Cl(1)···C(2) 3.277(5) Å. Stacking interactions between the ppy–ppy and 4-pyacH-4-pyacH ring system were observed (Figs. S4 and S5). The closest Pt···Pt distance for **4** is 5.332(4) Å eliminating the possibility of a Pt–Pt bond.

The 3D Hirshfeld surface of **4** is plotted over $d_{norm}$ (a) and 2D fingerprint plots from different contacts: (b) overall; (c) C···C/C···C (8.8 %); (d) C···H/C···H (15.4 %); (e) Cl···H/Cl···H (12.4 %) (Fig. S6). Similarly, to **3**, Cl···H contacts occupy the 12.4 % of the overall set of contacts, while the H···H contacts are 34.2 %.

### 3.3. Solution structural features of *1*–*4*

The $^1$H NMR spectrum of **1** was recorded in $CDCl_3$ due to its low solubility in all common NMR solvents. The spectrum consists of twelve signals suggesting that all the protons are non-equivalent. Characteristic $^3J_{Pt\text{-}H}$ satellites were observed for the ppyH3′ (34.0 Hz), ppyH6 (39.1 Hz), and 2-pyacHa (36.1 Hz) indicating that both ligands are coordinated. The chemical shifts of ppyH6 and 2-pyacHa appear at 9.21 and 9.23 ppm, shifted downfield by 0.55 and 0.97 ppm in comparison to the free ligands due to the coordination of the neighboring nitrogen atoms. Also, the ppyH3′ was observed at 7.50 ppm which is a typical value for N^C coordinated ppy [32]. In the NOESY spectrum of **1** a strong inter-

**Table 2**
Photophysical data of the complexes **1**–**4**.

| | Absorbance | Excitation | | Emission | | | |
|---|---|---|---|---|---|---|---|
| | | Solution | solid | Solution | | Solid | |
| | UV/Vis absorbance (320–450 nm), $\lambda^{max}$ [nm], ($\varepsilon \times 10^3$ [$M^{-1}$ $cm^{-1}$]) | $\lambda_{exc}$ [nm] | $\lambda_{exc}$ [nm] | $\lambda_{em}$ [nm] | Quantum yield (Q %) | $\lambda_{em}$ [nm] | Quantum yield (Q %) |
| **1** | 328 (5.0), 353 (6.8), 383 sh (1.6), 400 sh (1.5) | 367 | 385 | 492, 525, 552 sh | 0.16 | 498sh, 522, 568 | 3.20 |
| **2** | 326(5.9), 351(3.0), 388 sh (2.3), 400 sh (2.1) | 426 | – | 488, 524, 545 sh | 0.05 | – | – |
| **3** | 325 (4.7), 340 (4.0), 386 (1.8), 397 (1.8) | 385 | 385 | 487, 522, 547 sh | 0.17 | 503sh, 525, 555 | 3.55 |
| **4** | 327 (4.4), 352 (2.8), 384sh (1.9) | 371 | 385 | 488, 521, 564 sh | 0.15 | 503sh, 525, 555 | 4.86 |

ligand NOE connectivity between the ppyH3′ and 2-pyacH$_a$ confirms the coplanarity of the ppy and 2-pyacH rings (Fig. 5). However, the spectrum of **1** in acetone-$d_6$ shows very weak signals which could be unambiguously assigned only to the ppyH6 (9.10 ppm), 2-pyacHa (9.39 ppm) and ppyH3′ (7.62 ppm). Upon dissolution of the complex in acidified acetone-$d_6$, complex **2** was formed. A significant downfield shift (+0.63) was observed for the ppyH6 (9.73 ppm) while the 2-pyacHa was slightly shifted (9.43 ppm, +0.04 ppm), reflecting the opening of the 2-pyac NˆO chelate, the coordination of a chlorine to the platinum center and the interaction of ppyH6 with the coordinated chlorine. Also, the ppyH3′ shifted upfield by −1.09 ppm indicating that it was placed over the 2-pyacH aromatic ring. In this case, the 2-pyacH ring should be perpendicular to the ppy ring system. The characteristic platinum satellites were observed for the ppyH3′ (46.1 Hz), ppyH6 (39.1 Hz) and 2-pyacHa (44.3 Hz). In the NOESY spectrum of **2** in acidified acetone-$d_6$, the NOE connectivity between the ppyH3′ and 2-pyacHa vanished, indicating the vertical orientation of the 2-pyacH pyridine ring towards the ppy aromatic system (Fig. 5).

In the $^1$H NMR spectrum of **3** twelve signals appeared, indicating that all protons of the complex are non-equivalent. The characteristic $^3J_{Pt\text{-}H}$ coupling was observed for the ppyH3′ (41.0 Hz), ppyH6 (38.1 Hz), 3-pyacHa (48.3 Hz) and 3-pyacHe (45.4 Hz) indicating that both ligands are coordinated to the platinum center. The values of $^3J$ are within the range of similar complexes [33]. However, a remarkable downfield shift for the ppyH6 (9.81 ppm, +1.13) was observed reflecting the sum of the shifts due to the ppyN1 coordination and the interaction with the neighboring chlorine. On the other hand, the protons of the 3-pyacH pyridine ring 3-pyacHa (9.63 ppm) and 3-pyacHe (9.32 ppm) shifted less downfield, at about +0.40 ppm, due to the 3-pyacH coordination, as expected. Also, the ppyH3′ was observed significantly upfield (6.39 ppm), affected by the π-aromatic ring of 3-pyacH due to its relative orientation towards the ppy plane. The latter was also confirmed from the NOESY spectrum of **3**, where two weak NOE connectivities between ppyH3′ and both 3-pyacHa and 3-pyacHe were observed (Fig. 5).

Similarly, in the spectrum of **4** ten signals were observed. The signals of Ha and He as well as those of Hb and Hd appeared to be equivalent due to the symmetric nature of 4-pyacH. Additionally, eight signals of the ppy protons were observed. Thus, the characteristic $^3J_{Pt\text{-}H}$ coupling was found for three signals, ppyH3′ (44.3 Hz), ppyH6 (36.5 Hz), and 3-pyacHe/Ha (43.5 Hz) indicating that both ligands are coordinated to the platinum center. As in the case of **3** a downfield shift for the ppyH6 (9.72 ppm) was observed suggesting a strong interaction with the neighboring Cl. The signal of 4-pyacHa/He was found downfield (9.22 ppm) as expected. Once again, the perpendicular orientation of the 4-pyacH pyridine ring towards the ppy plane influenced the chemical shift of the ppyH3′, which was observed significantly upfield (6.42 ppm). In the NOESY spectrum of **4**, apart from the intra-ligand NOEs, a weak NOE connectivity between the ppyH3′ equivalent 4-pyacHa/He confirms the relative vertical orientation of the 4-pyacH ring (Fig. 5).

In conclusion, for complexes **1**–**4** solution structural features can be extracted from the $^1$H NMR spectroscopical data and may be compared with their crystal structures. The $^1$H NMR chemical shift of ppyH3′ is a good indicator for the relative positions of ppy and carboxy pyridine planes since ppyH3′ is located over the carboxy pyridine aromatic ring. Thus, in the complexes **1**–**4** ppyH3′ varied from 7.62 to 6.30 ppm, reflecting the torsion angle (γ) between the planes of the carboxy pyridine and ppy. The more downfield the observed shift, the more γ tends to zero [**1**: 7.62 ppm, γ is almost zero] [10] and conversely the more upfield it was the more γ tends to 90° [**3**: 6.39 ppm, γ is about 80° (average from A and B forms); **4** 6.42 ppm, γ is about 65°]. In the case of complex **2**, where no crystal structure was achieved, the ppyH3′ was observed at 6.30 ppm which may indicate a vertical orientation (γ = 90°) of the 2-pyacH ring towards the ppy ring system. In this position an axial interaction between 2-pyacH carboxylic group and platinum center may be facilitated. The NOESY spectra of the complexes are also informative, while in the case of **2** no NOE connectivity between the 2-pyacH and ppyH3′ was observed, confirming its orientation towards the ppy plane. The interactions between the Cl(1) and the ppyH6, which were observed in the crystal structures of **3** and **4**, were retained in the solution as well, since in these complexes the H6′ is significantly shifted compared to **1**.

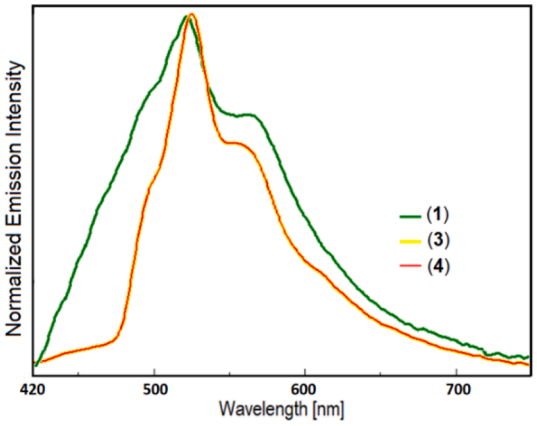


**Fig. 6.** Intensity-normalized solid-state emission spectra of **1**, **3** and **4** at room temperature ($\lambda_{exc}$ = 385 (**1**, **3**, **4**)).

### 3.4. Absorption and emission spectra of the complexes

The photophysical data of the complexes **1**–**4** are summarized in Table 2. Solid state emission spectra for **1**, **3** and **4** are presented in Fig. 6 while the absorption spectra are presented in Fig. S15. All studied complexes show steady-state electronic spectra which are similar to each other. The weak absorption bands at about 380–400 nm with molar coefficients (ε) varied from 1500 to 2200 $M^{-1}cm^{-1}$ are assigned to metal-to-ligand charge-transfer (MLCT) [34]. Moderate absorption bands at 325–355 nm (ε = 3000–6800 $M^{-1}$ $cm^{-1}$) are assigned to

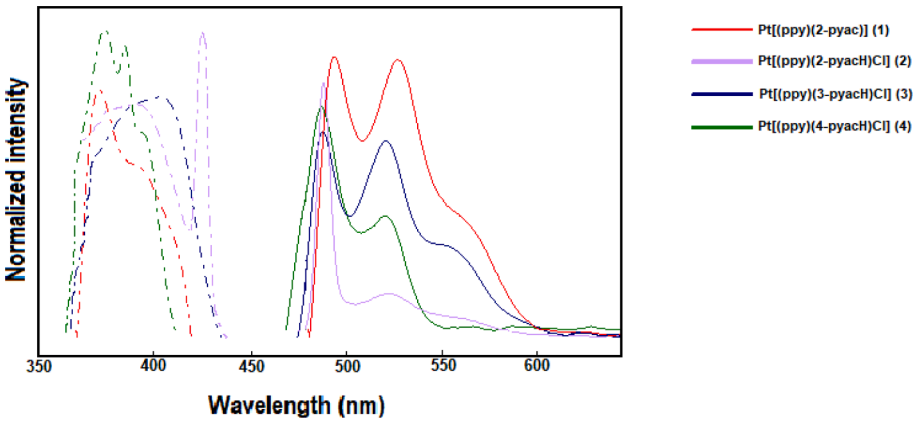


**Fig. 7.** Intensity-normalized solution emission and excitation (dotted lines) spectra of **1**–**4** (C = 3.9 × $10^{-4}$ M) in degassed acetone at room temperature ($\lambda_{exc}$ = 367, 426, 385, 371 for **1**, **2**, **3**, **4** respectively).

transitions 5d(Pt) → π*(L) [35]. In the case of **1** the transition 5d(Pt) → π*(L) at 353 nm has the higher ε (6800 $M^{-1}$ $cm^{-1}$) among the studied complexes reflecting the difference of **1** from **2** to **4** due to the chelating (N, O) action of 2-pyacH.

Upon excitation of the complexes at 380–385 nm in the solid-state, a green emission centered about 530 nm with $\Phi$ varied from 3.20 to 4.86 was produced. The spectra appeared almost the same for **3** and **4** while complex **1** exhibited its emission bands slightly shifted to red.

The emission and excitation (dotted lines) spectra of **1**–**4** in degassed solution of acetone are shown in Fig. 7.

Upon excitation of the complexes a green emission was produced with a very low quantum yield ($\Phi$ ~ 0.05–0.17 %), as expected. All complexes emitted similarly in the range of 475–580 nm while complex **2** was almost non-emissive ($\Phi$ ~ 0.05). The emission spectra of (**2**) and (**3**) in acetone solution (3.9 × $10^{-4}$) show a vibronic structure with vibronic spacing of 1408 and 735 $cm^{-1}$ for (**2**), and 1376 and 876 $cm^{-1}$ for (**3**), due to the high energy vibrations of ppy. In the case of (**4**) only a spacing of 1298 $cm^{-1}$ is observable. The above results are consistent with emission derived from the triplet excited states, mixed with $^3$MLCT and $^3$IL [36–38].

## 4. Conclusions

Mixed ligand cyclometalated Pt(II) complexes with 2-phenylpyridine (ppyH) and the pyridine carboxylic acids (PCAs), picolinic (2-pyacH), nicotinic (3-pyacH) and isonicotinic (4-pyacH) acid, with the general formula *trans-N,N*-[Pt(ppy)(PCA)Cl] [PCA = 2-pyacH (**2**), 3-pyacH (**3**), 4-pyacH (**4**)] were synthesized and characterized in solid state and in solutions of acetone. Complexes (**3**) and (**4**) are consistent with the assumption that the *trans*-influence of the strong σ-bonded carbon atom of ppy lengthens the *trans*-(Pt–Cl) bond, due to an electrostatic repulsion from the platinum $d_\pi$ electron density towards the chloride ligand [39]. Also, the orthometalated ppyC2′ influences the $^3J_{Pt\text{-}H}$ value of the co-ordinated pyridine rings. Thus, the ppyH6 (*cis*- to ppyC2′) is always smaller than the $pyacH_{(a/e)}$ (*trans*- to ppyC2′), with a ratio ranging from 0.80 to 0.88. The crystal structure of the complexes **3** and **4** showed that 3-pyacH and 4-pyacH coordinated through the pyridinic nitrogen atom, forming hydrogen-bonded homodimers through their carboxylic groups. Solution-structural features of the complexes **2**–**4** revealed that the dihedral angle (γ) between the PCA plane and the plane of ppy depends on the carboxylic substitution of the pyridine ring and in the cases of **3** and **4** the solid-state characteristics were retained. All complexes emit in degassed solutions of acetone (475–580 nm) with a very low quantum yield ($\Phi$ ~ 0.05–0.17 %), while in the solid state, a green emission centered at about 530 nm with $\Phi$ varying from 3.20 to 4.86 % was produced.

## CRediT authorship contribution statement

**Evangelia Sifnaiou:** Conceptualization, Methodology, Writing – original draft, Writing – review & editing, Investigation. **Antonia Garypidou:** Conceptualization, Writing – original draft, Investigation. **Konstantinos Ypsilantis:** Visualization, Investigation, Conceptualization. **John C. Plakatouras:** Methodology, Formal analysis, Writing – review & editing. **Achilleas Garoufis:** Supervision, Writing – review & editing.

## Declaration of Competing Interest

The authors declare that they have no known competing financial interests or personal relationships that could have appeared to influence the work reported in this paper.

## Data availability

No data was used for the research described in the article.

## Acknowledgments

Evangelia Sifnaiou, Antonia Garypidou and Konstantinos Ypsilantis were financially supported by the program “PERIFEREIAKI ARISTEIA” (Regional Excellence) co-financed by the European Union and the Hellenic Republic Ministry of development and investments under NSRF 2014-2020 (Region of Epirus, call 111 MIS 5047233, MIS 5047235). We also acknowledge the X-ray Center of single crystal diffraction, the Unit of Environmental, Organic and Biochemical high-resolution analysis-ORBITRAP-LC-MS and the NMR Center of the University of Ioannina for providing access to the facilities.

## Appendix A. Supplementary data

Supplementary data to this article can be found online at https://doi.org/10.1016/j.poly.2022.116252.

## References

[1] H. Yersin, A.F. Rausch, R. Czerwieniec, T. Hofbeck, T. Fischer, The triplet state of organo-transition metal compounds. Triplet harvesting and singlet harvesting for efficient OLEDs, Coord. Chem. Rev. 255 (2011) 2622–2652, https://doi.org/10.1016/j.ccr.2011.01.042.

[2] L. Flamigni, A. Barbieri, C. Sabatini, B. Ventura, F. Barigelletti, Photochemistry and photophysics of coordination compounds: iridium, in: Photochem. Photophysics Coord. Compd. II, Springer Berlin Heidelberg, Berlin, Heidelberg, n.d., pp. 143–203. 10.1007/128_2007_131.

[3] J.A.G. Williams, Photochemistry and photophysics of coordination compounds: platinum, in: Photochem. Photophysics Coord. Compd. II, Springer Berlin Heidelberg, Berlin, Heidelberg, n.d., pp. 205–268. 10.1007/128_2007_134.
[4] Y. Chi, P.-T. Chou, Transition-metal phosphors with cyclometalating ligands: fundamentals and applications, Chem. Soc. Rev. 39 (2010) 638–655, https://doi.org/10.1039/B916237B.
[5] A. Abhervé, M. Mastropasqua Talamo, S. Boi, V. Poupard, F. Gendron, B. Le Guennic, N. Avarvari, F. Pop, Thiophene-bipyridine appended diketopyrrolopyrrole ligands and platinum(II) complexes, Inorg. Chem. 60 (2021) 7351–7363, https://doi.org/10.1021/acs.inorgchem.1c00534.
[6] J. Ni, W. Zheng, W.J. Qi, Z.C. Guo, S.Q. Liu, J.J. Zhang, Synthesis, structure and luminescent switching properties of cycloplatinated(II) complexes bearing phenyl β-diketone ligands, J. Organomet. Chem. 952 (2021), 122048, https://doi.org/10.1016/j.jorganchem.2021.122048.
[7] L. Gao, J. Ni, M. Su, J. Kang, J. Zhang, Luminescence switching property of cycloplatinated(II) complexes bearing 2-phenylpyridine derivatives and the application for data security storage, Dye Pigm. 165 (2019) 231–238, https://doi.org/10.1016/j.dyepig.2019.02.004.
[8] J. Kalinowski, V. Fattori, M. Cocchi, J.A.G. Williams, Light-emitting devices based on organometallic platinum complexes as emitters, Coord. Chem. Rev. 255 (2011) 2401–2425, https://doi.org/10.1016/j.ccr.2011.01.049.
[9] J. Brooks, Y. Babayan, S. Lamansky, P.I. Djurovich, I. Tsyba, R. Bau, M. E. Thompson, Synthesis and characterization of phosphorescent cyclometalated platinum complexes, Inorg. Chem. 41 (2002) 3055–3066, https://doi.org/10.1021/ic0255508.
[10] M. Ebina, A. Kobayashi, T. Ogawa, M. Yoshida, M. Kato, Impact of a carboxyl group on a cyclometalated ligand: hydrogen-bond- and coordination-driven self-assembly of a luminescent platinum(II) complex, Inorg. Chem. 54 (2015) 8878–8880, https://doi.org/10.1021/acs.inorgchem.5b01343.
[11] A.I. Solomatina, A.D. Slobodina, E.V. Ryabova, O.I. Bolshakova, P.S. Chelushkin, S. V. Sarantseva, S.P. Tunik, Blood-brain barrier penetrating luminescent conjugates based on cyclometalated platinum(II) complexes, Bioconjug. Chem. 31 (2020) 2628–2637, https://doi.org/10.1021/acs.bioconjchem.0c00542.
[12] G. Millán, N. Giménez, R. Lara, J.R. Berenguer, M.T. Moreno, E. Lalinde, E. Alfaro-Arnedo, I.P. López, S. Pineiro-Hermida, J.G. Pichel, Luminescent cycloplatinated complexes with biologically relevant phosphine ligands: optical and cytotoxic properties, Inorg. Chem. 58 (2019) 1657–1673, https://doi.org/10.1021/acs.inorgchem.8b03211.
[13] J. Kang, R. Zaen, K.-M. Park, K.H. Lee, J.Y. Lee, Y. Kang, Cyclometalated platinum (II) β-diketonate complexes as single dopants for high-efficiency white OLEDs: the relationship between intermolecular interactions in the solid state and electroluminescent efficiency, Cryst. Growth Des. 20 (2020) 6129–6138, https://doi.org/10.1021/acs.cgd.0c00838.
[14] M. Vaquero, N. Busto, N. Fernández-Pampín, G. Espino, B. García, Appended aromatic moieties determine the cytotoxicity of neutral cyclometalated platinum (II) complexes derived from 2-(2-pyridyl)benzimidazole, Inorg. Chem. 59 (2020) 4961–4971, https://doi.org/10.1021/acs.inorgchem.0c00219.
[15] S.A. Katkova, I.I. Eliseev, A.S. Mikherdov, E.V. Sokolova, G.L. Starova, M. A. Kinzhalov, Cyclometalated platinum(II) complexes with nitrile and isocyanide ligands: synthesis, structure, and photophysical properties, Russ. J. Gen. Chem. 91 (2021) 393–400, https://doi.org/10.1134/S1070363221030099.
[16] K.S. Kisel, A.S. Melnikov, E.V. Grachova, P. Hirva, S.P. Tunik, I.O. Koshevoy, Linking Re I and Pt II chromophores with aminopyridines: a simple route to achieve a complicated photophysical behavior, Chem. Eur. J. 23 (2017) 11301–11311, https://doi.org/10.1002/chem.201701539.
[17] N. Ghavale, A. Wadawale, S. Dey, V.K. Jain, Synthesis, structures and spectroscopic properties of platinum complexes containing orthometalated 2-phenylpyridine, J. Organomet. Chem. 695 (2010) 1237–1245, https://doi.org/10.1016/j.jorganchem.2010.01.035.
[18] APEX 3, SAINT, SHELXT, Bruker AXS Inc., 5465 East Cheryl Parkway, Madison, 2016.
[19] G.M. Sheldrick, SADABS, University of Göttingen, Germany, 1996.
[20] G.M. Sheldrick, Crystal structure refinement with SHELXL, Acta Crystallogr. Sect. C: Struct. Chem. 71 (2015) 3–8, https://doi.org/10.1107/S2053229614024218.
[21] C.B. Hübschle, G.M. Sheldrick, B. Dittrich, ShelXle: a Qt graphical user interface for SHELXL, J. Appl. Cryst. 44 (2011) 1281–1284, https://doi.org/10.1107/S0021889811043202.
[22] A.L. Spek, Structure validation in chemical crystallography, Acta Crystallogr. D: Biol. Crystallogr. 65 (2009) 148–155, https://doi.org/10.1107/S090744490804362X.
[23] L.J. Barbour, X-Seed – a software tool for supramolecular crystallography, J. Supramol. Chem. 1 (2001) 189–191, https://doi.org/10.1016/S1472-7862(02)00030-8.
[24] P.R. Spackman, M.J. Turner, J.J. McKinnon, S.K. Wolff, D.J. Grimwood, D. Jayatilaka, M.A. Spackman, CrystalExplorer : a program for Hirshfeld surface analysis, visualization and quantitative analysis of molecular crystals, J. Appl. Cryst. 54 (2021) 1006–1011, https://doi.org/10.1107/S1600576721002910.
[25] N. Godbert, T. Pugliese, I. Aiello, A. Bellusci, A. Crispini, M. Ghedini, Efficient, ultrafast, microwave-assisted syntheses of cycloplatinated complexes, Eur. J. Inorg. Chem. 2007 (2007) 5105–5111, https://doi.org/10.1002/ejic.200700639.
[26] A. Garypidou, K. Ypsilantis, T. Tsolis, A. Kourtellaris, J.C. Plakatouras, A. Garoufis, Synthesis and characterization of mixed ligand cyclopalladates with 2-phenylpyridine and substituted phenanthrolines: investigation into the hydroxylation reaction of 2-phenylpyridine, Inorg. Chim. Acta 518 (2021), 120254, https://doi.org/10.1016/j.ica.2021.120254.
[27] W.B. Wright, G.S.D. King, The crystal structure of nicotinic acid, Acta Crystallogr. 6 (1953) 305–317, https://doi.org/10.1107/S0365110X53000867.
[28] S. Long, M. Siegler, T. Li, 6-Chloronicotinic acid, Acta Crystallogr. Sect. E: Struct. Rep. Online 63 (2007) o279–o281, https://doi.org/10.1107/S1600536806053177.
[29] V.A. Blatov, A.P. Shevchenko, D.M. Proserpio, Applied topological analysis of crystal structures with the program package ToposPro, Cryst. Growth Des. 14 (2014) 3576–3586, https://doi.org/10.1021/cg500498k.
[30] M.A. Spackman, D. Jayatilaka, Hirshfeld surface analysis, CrstEngComm 11 (2009) 19–32, https://doi.org/10.1039/B818330A.
[31] R. Sekiya, S. Nishikiori, A preparative strategy for supramolecular inclusion compounds by combination of dimer formation of isonicotinic acid and coordination bonding, Chem. Commun. (2001) 2612–2613, https://doi.org/10.1039/b108458e.
[32] L. Pazderski, J. Toušek, J. Sitkowski, L. Kozerski, E. Szłyk, 1H, 13C and 15N nuclear magnetic resonance coordination shifts in Au(III), Pd(II) and Pt(II) chloride complexes with phenylpyridines, Magn. Reson. Chem. 47 (2009) 658–665, https://doi.org/10.1002/mrc.2445.
[33] B.M. Still, P.G.A. Kumar, J.R. Aldrich-Wright, W.S. Price, 195Pt NMR—theory and application, Chem. Soc. Rev. 36 (2007) 665–686, https://doi.org/10.1039/B606190G.
[34] Á. Díez, J. Forniés, S. Fuertes, E. Lalinde, C. Larraz, J.A. López, A. Martín, M. T. Moreno, V. Sicilia, Synthesis and luminescence of cyclometalated compounds with nitrile and isocyanide ligands, Organometallics 28 (2009) 1705–1718, https://doi.org/10.1021/om800845c.
[35] S.C.F. Kui, F.-F. Hung, S.-L. Lai, M.-Y. Yuen, C.-C. Kwok, K.-H. Low, S.-S.-Y. Chui, C.-M. Che, Luminescent organoplatinum(II) complexes with functionalized cyclometalated C^N^C ligands: structures, photophysical properties, and material applications, Chem. Eur. J. 18 (2012) 96–109, https://doi.org/10.1002/chem.201101880.
[36] S.-W. Lai, H.-W. Lam, W. Lu, K.-K. Cheung, C.-M. Che, Observation of low-energy metal–metal-to-ligand charge transfer absorption and emission: electronic spectroscopy of cyclometalated platinum(II) complexes with isocyanide ligands, Organometallics 21 (2002) 226–234, https://doi.org/10.1021/om0106276.
[37] W. Lu, M.C.W. Chan, N. Zhu, C.-M. Che, C. Li, Z. Hui, Structural and spectroscopic studies on Pt···Pt and π−π interactions in luminescent multinuclear cyclometalated platinum(II) homologues tethered by oligophosphine auxiliaries, J. Am. Chem. Soc. 126 (2004) 7639–7651, https://doi.org/10.1021/ja039727o.
[38] W. Lu, B.-X. Mi, M.C.W. Chan, Z. Hui, C.-M. Che, N. Zhu, S.-T. Lee, Light-emitting tridentate cyclometalated platinum(II) complexes containing σ-alkynyl auxiliaries: tuning of photo- and electrophosphorescence, J. Am. Chem. Soc. 126 (2004) 4958–4971, https://doi.org/10.1021/ja0317776.
[39] L.J. Manojlovic-Muir, K.W. Muir, The trans-influence of ligands in platinum(II) complexes. The significance of the bond length data, Inorg. Chim. Acta 10 (1974) 47–49, https://doi.org/10.1016/S0020-1693(00)86707-9.